

# Turbo-coded Multi-alphabet Binary CPM for Concatenated Continuous Phase Modulation

Jun Ning, Minyue Fu and Graham Wade

School of EECS, University of Newcastle, NSW 2308 Australia

Emails: jun.ning@studentmail.newcastle.edu.au; minyue.fu@newcastle.edu.au

**Abstract**—Constant envelope and high spectral efficiency are among the key properties which make continuous phase modulation (CPM) a preferred choice for many applications. Numerous methods are available for designing concatenated CPM systems to achieve additional coding gains. In this paper, we propose a new serial concatenated CPM scheme. Our design uses a multi-alphabet binary CPM as an inner code, a modified turbo code as an outer code, and specially designed interleavers. The extrinsic information transfer (EXIT) chart technique has been employed to assist the outer code design. Using soft decision decoding, we show that our design gives noticeable improvements compared with previous concatenated CPM schemes over additive white Gaussian noise (AWGN) channel.

**Keywords:** Continuous phase modulation; turbo code; concatenated continuous phase modulation; serial concatenated code.

## I. INTRODUCTION

Continuous phase modulation (CPM) has several good properties which make it a preferred modulation scheme for radio and satellite communications. Among these properties are constant envelope, spectral efficiency and inherent coding; see, e.g., [1], [2].

CPM is a coded modulation scheme that can be decomposed into a recursive continuous phase encoder (CPE) and a memoryless mapper (MM) [3]. The CPE provides the inherent code trellis, which in turn depends upon the CPM design parameters. These include the modulation index,  $h = 2k/p$ , where  $k$  and  $p$  are relatively prime positive integers. Other parameters are the frequency pulse  $g(t)$ , the duration,  $L$ , of the frequency pulse, the size of the data alphabet,  $M$ , and the symbol period,  $T$ . Usually,  $M = 2, 4$  or  $8$ , and  $L$  is between 1 and 3 symbol periods. These parameters are usually chosen to satisfy a given bandwidth specification, which in turn limits the bit error rate (BER) performance of the inherent code. A common solution is to improve the power efficiency by using the serial concatenated scheme in Fig. 1; see, e.g., [5], [8]. If  $R_o$  is the rate of the outer code, the rate of this scheme is  $R = R_o \log_2 M$  bits/symbol. When the outer code is a simple convolutional code, the scheme becomes the serial concatenated convolutional coded (SCCC) system described in [6] and advantages can be taken from the recursive nature of the CPE. Iterative decoding can give large coding gains at the expense of the interleaver delay. Another approach is to enhance the distance spectrum of the CPM signal by combining the CPE with an inner code of rate  $R_i$ , giving an overall rate  $R = R_o R_i \log_2 M$  bits/symbol. Ideally, both inner and outer codes operate over the same algebraic field so that

no symbol mapping is required, and also the inner code can be combined with the CPE in the trellis coded modulation sense [4]. Simulation shows that the use of non-binary outer encoder can give typically 0.3dB improvement for 4CPFSK,  $h = 1/4$ . A suboptimal design technique would be to maximize the minimum Euclidean distance of the combined inner code. Disadvantages of this scheme are 1) optimization of the outer code is difficult, and 2) non-binary codes are more difficult to handle.

In this paper, we adopt the basic serial configuration in Fig. 1 but with a turbo code, i.e., parallel concatenated convolutional code (PCCC), as the outer code. Also, a modified binary CPM encoder is used as the inner code, illustrated in Fig. 2. This has the advantage of binary coding throughout, together with increased power in the outer code. Turbo coded CPM using soft iterative decoding has been described in [10], [12]. However, multiple CPM channels are required in [10] to implement the turbo coded CPM. More specifically, [10] concatenates two CPM channels with a turbo code and shows that some small improvement can be achieved. The use of multiple CPM channels makes it easier to consider turbo codes. However, this approach has two drawbacks. Firstly, it complicates the modulation scheme. Secondly, implementing multiple CPM channels on a given frequency band may not be realistic. The scheme in [12] is closely related to our scheme. However, we focus on binary CPM with full response whereas [12] is concerned with 8-ary CPM system with partial response. It turns out that the outer code design depends significantly on different CPM systems.

When employing a PCCC as an outer code, a naive approach would be to modify a standard PCCC scheme by replacing the binary phase shift keying (BPSK) with a CPM. However, it is shown by simulation that such an approach would not perform well. Even when an additional interleaver (called a concatenation interleaver) is inserted before the CPM, the improvement in the performance is still limited. Motivated by this fact, the key question we address in this paper is how to make a PCCC based concatenated CPM scheme work. It turns out that this involves careful design of all the individual components of the system, including the outer code, the inner code and the concatenation interleaver, as described below.

Firstly, due to the recursive property of CPM, the PCCC we use differs from a standard PCCC with BPSK modulation in that our constituent encoders for the PCCC are non-recursive. It turns out that for serially concatenated CPM, non-

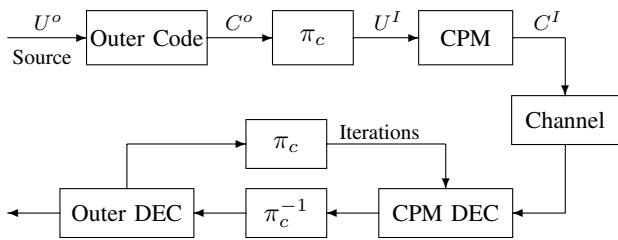


Fig. 1. Serial concatenated CPM scheme

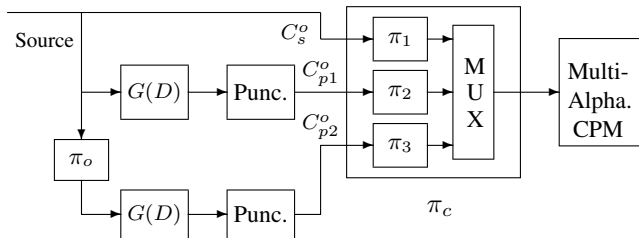


Fig. 2. Proposed concatenated CPM scheme

recursive constituent encoders give a significant improvement compared with recursive ones at low signal-to-noise ratio (SNR). Secondly, in order to match the binary outer code, the inner code (CPM) is chosen to be a binary CPM. However, to strengthen the Euclidean distance of the inner encoder, we deploy a multi-alphabet binary CPM. It is known [1], [2] that multi- $h$  CPM has better distance and memory properties than a single- $h$  CPM. A multi-alphabet binary CPM is similar to, but somewhat more general than, a multi- $h$  binary CPM. It offers more flexibility and gives similar improvements in these properties with same or lower complexity. Finally, the concatenation interleaver we use is chosen to both decorrelate the inner and outer code sequences and maintaining the independence of the two constituent code sequences in the outer code. This is an important property for the successful decoding of the PCCC outer code. Indeed, although a generic interleaver may de-correlate the inner and outer codes well, it would seriously correlate the constituent code sequences, weakening the purpose of using a PCCC.

We have compared our designs with previously available results on concatenated CPM. Simulations are conducted for AWGN channels. Our scheme achieves about 0.5 dB improvement at bit error rate (BER) of  $10^{-5}$  when overall coding rate  $R = 1/2$ .

The rest of this paper is organized as follows: Section II proposes the new concatenated CPM scheme. Section III discusses the soft decision decoding algorithm used in our study. Section IV shows some simulations and comparisons and Section V concludes the paper.

## II. A NEW CONCATENATED CPM SCHEME

The proposed scheme is depicted in Fig. 2, where only the encoding part is shown. The outer code is a binary PCCC. The systematic bit sequence and parity bit sequences (possibly punctured) are sent to a concatenation interleaver  $\pi_c$

to produce bit sequence for the inner code which is a multi-alphabet binary CPM. In the following, we detail the design of each component in the system.

### A. Inner Code

Binary CPM is by far the simplest CPM scheme. It is easier to understand and simpler to implement than other CPM schemes with a higher  $M$  value. However, CPM schemes with a higher  $M$  value have the advantage of allowing the outer code to have a lower coding rate, thus having the potential to offer a better overall coding gain. Indeed, since the overall coding rate is given by  $R = R_o \log_2 M$ , a higher  $M$  permits a lower  $R_o$  for the same  $R$ . The tradeoff is the design complexity and decoding complexity, i.e., a system with a higher  $M$  and lower  $R_o$  is more complex to design and decode.

Recall that a baseband CPM signal can be expressed as

$$s(t) = \exp(j\phi(t, \mathbf{I}))$$

where

$$\phi(t, \mathbf{I}) = 2\pi \sum_{k=-\infty}^n I_k h_k q(t - kT), \quad nT \leq t < (n+1)T$$

$T$  is the symbol period,  $\{I_k\}$  is the sequence of  $M$ -ary information symbols taken from the alphabet set  $\Lambda = \{\pm 1, \pm 3, \dots, \pm(M-1)\}$ ,  $M \geq 2$  is an even number,  $\{h_k\}$  is a sequence of modulation indices and  $q(t)$  the phase pulse which is the integrate of the frequency pulse  $g(t)$ , with  $q(T) = 1/2$ . A single- $h$  CPM has a constant  $h_k$  (or  $h$ ) whereas a multi- $h$  CPM uses a periodic  $h_k$ . Note that the average phase change is given by  $Mh_k\pi/2$ .

A multi-alphabet CPM is a simple generalization of the multi- $h$  scheme. Instead of varying  $h$ , we may vary the alphabet set, i.e., we use a periodic  $\Lambda_k$  instead of a constant  $\Lambda$ . As in the multi- $h$  scheme, the purpose of this CPM is to increase the Euclidean distance. But this is achieved by varying the possible phase increments in the alphabets rather than the modulation index. It is obvious that any multi- $h$  CPM can be regarded as a multi-alphabet CPM. The converse is not necessarily true. This is due to the fact that, for the multi-alphabet CPM, the difference between any two different symbols is not necessary to be an even number. Thus, multi-alphabet CPM schemes are more flexible than multi- $h$  CPM schemes. We note that the multi-alphabet CPM scheme is somewhat similar to the so-called generalized asymmetric multi- $h$  CPM scheme in [13] where the  $h$  value depends on both the time and the value of the input symbol.

The multi-alphabet binary CPM we propose to use in this paper has the following parameters: rectangular frequency pulse,  $h = 2k/p = 1/4$ , the alphabets alternate between  $\Lambda_1 = \{2, -2\}$  and  $\Lambda_2 = \{1, -2\}$ . It is obvious that this CPM has a periodic trellis and the cardinality of the multi-alphabet binary CPM (or the effective value of  $M$ ) is still equal to 2. As the value of a symbol may equal 2 or  $-2$ , the  $h$  is chosen to be  $1/4$  in order to remain the CPM bandwidth same or almost same with that of Minimum-Shift Keying (MSK) which has a symbol alphabet  $\Lambda = \{1, -1\}$ .

Given  $\Lambda_1 = \{2, -2\}$ , the  $\Lambda_2 = \{1, -2\}$  alphabet is used in preference to the  $\Lambda_1 = \{1, -1\}$  in order to maximize the minimum Euclidean distance. For a full response CPM, the number of possible phase states in the time-varying phase state trellis equals  $p$ , over two adjacent symbol periods. A higher number of the states means a higher system complexity. MSK has 4 possible states in the trellis and its minimum Euclidean distance is equal to 2.0 (see [1], [2]). It is verified that the multi-alphabet binary CPM above has 8 possible states and its minimum Euclidean distance roughly equals 3.1. Obviously, the multi-alphabet binary CPM achieves the higher minimum Euclidean distance at expense of the complexity. The minimum Euclidean distance, 3.1, can also be achieved by a multi- $h$  binary CPM with same bandwidth. But the number of states required is doubled, i.e.,  $p = 16$ , compared with that of the multi-alphabet binary CPM. This demonstrates the advantage of using the multi-alphabet binary CPM when trying to increase the minimum Euclidean distance without bandwidth expansion.

It is known that the power spectrum of CPM is largely determined by the average phase change per symbol period  $T$ , provided that  $L$  and the shape function are fixed [2], [11]. This is especially true when the maximum phase change is fixed. For a single- $h$  CPM, the average phase change is given by  $Mh\pi/2$ . Since MSK has  $M = 2$  and  $h = 1/2$ , the average phase change is  $\pi/2$  which equals the maximum phase change. For a multi- $h$  binary CPM, the average phase is  $\bar{h}\pi$ , where  $\bar{h}$  is the average value of  $h$ . For our multi-alphabet binary CPM, the average phase change is easily verified to be  $7\pi/16$  which is slightly smaller than the maximum phase change,  $\pi/2$ . Thus, it is expected that the generalized multi- $h$  binary CPM possesses a slightly narrower bandwidth than MSK. Indeed, simulations show that the former two schemes have very comparable power spectra (Details are not shown in this paper).

### B. Outer Code Design and EXIT Charts

As mentioned above, the outer code is a binary PCCC. However, there is a main difference in the constituent encoder  $G(D)$ . A normal PCCC uses a recursive  $G(D)$  to ensure that if one parity bit sequence exhibits a low weight, the other is likely to have a higher weight. Here, we find that at relatively high BER, a non-recursive code  $G(D)$  can perform better. This may be due to the fact that for a normal PCCC the associated modulation is a memoryless BPSK, whereas in our case the CPM is already a recursive encoder. In fact, the concatenation of a PCCC and CPM can be regarded as two serially concatenated codes connected in parallel, and then merged into the inner CPM code. Thus, the combination of each constituent encoder  $G(D)$  and the CPE can be viewed as a "local" serial concatenated code and the CPE has the recursion property.

To assist the design of the outer code, we may evaluate the decoding performance of the concatenated scheme at low signal-to-noise ratios using the so-called EXIT charts [15], [16]. With multi-alphabet binary CPM acting as the inner

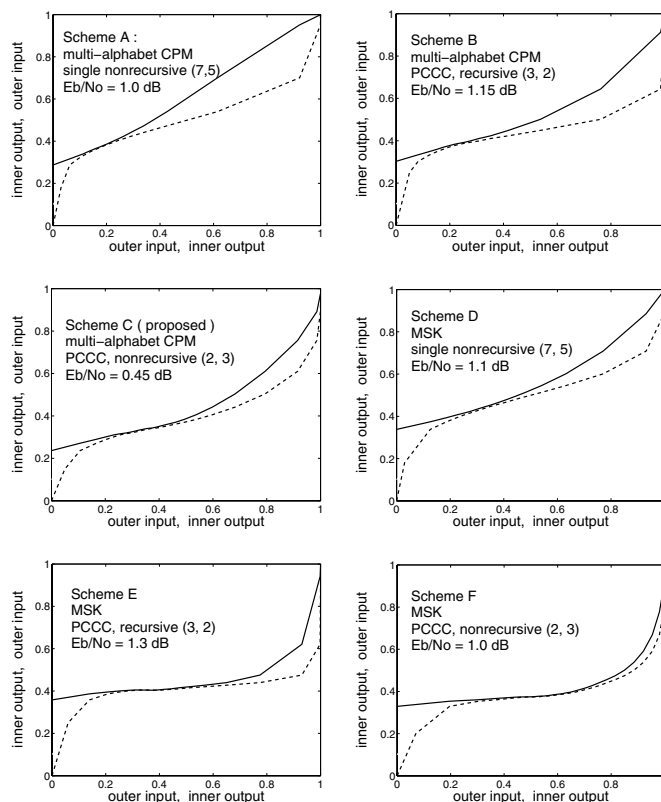


Fig. 3. EXIT charts of concatenated CPM systems

code, we consider three structures for rate-1/2 outer codes: a single convolutional code, a PCCC with a recursive constituent code and a PCCC with a nonrecursive constituent code. These schemes are referred to as schemes A, B and C, respectively. For PCCC, the first constitute code is terminated whereas the second one is not, and the parity bits are punctured to give an overall code rate of 1/2. The interleaver in Scheme A and the interleavers  $\pi_o$  in Schemes B and C are S-random. The concatenation interleavers for Schemes B and C will be discussed shortly. The input information block has 20,000 bits. The EXIT charts shown in Fig. 3 are computed using the approach in [14] which is based on [15], [16], [17]. For each scheme, the outer code is optimized by varying its generator polynomial and memory size so that the  $E_b/N_0$  threshold for decoding convergence is minimized. For Scheme A, the best outer code is a 4-state nonrecursive convolutional code with generator polynomial (7, 5) (octal). For Scheme B, the optimal outer code is a 2-state recursive convolutional code with generator polynomial (3, 2). These two schemes have convergence thresholds around 1.0 dB. For Scheme C, the threshold can be minimized to about 0.45 dB when the outer code is a PCCC with constituent code being the nonrecursive convolutional code (2, 3).

For comparison purposes, we also plot the EXIT charts in Fig. 3 for the schemes with MSK as the inner code. Replacing the multi-alphabet CPM by MSK in the schemes A, B and C, we obtain the schemes D, E and F. We can see clearly from

Fig. 3 that the proposed scheme (scheme C) offers the lowest (best) convergence threshold.

### C. Concatenation Interleaver

The primary role of the concatenation interleaver  $\pi_c$  is to de-correlate the inner code from the outer code, thus giving some interleaving gain. However, we have observed that a generic interleaver does not work effectively. Indeed, if the two constituent codeword sequences of the outer code are interleaved with each other, they will be strongly correlated after the inner coding. This would cause a serious problem for the outer decoding because a PCCC heavily relies on the independence of the constituent codeword sequences. Due to the observation above, the concatenation interleaver is chosen to include three sub-interleavers ( $\pi_1, \pi_2$  and  $\pi_3$ ), one for the systematic bit sequence and one for each of the parity bit sequences. The three interleaved bit sequences are then multiplexed together as the input to the inner code. The best multiplexing turns out to be the one which starts with the first parity bit sequence, followed by the systematic bit sequence, and then by the second parity bit sequence. Obviously, the two parity bit sequences can be swapped. The sub-interleavers are chosen to be  $S$ -random.

## III. DECODING

We employ iterative soft decision decoding in this paper. The basic idea of decoding follows from [7], [9]. The unique feature of our decoding problem is that there are effectively three constituent encoders in the system: two from the PCCC and the third one being the inner code. It turns out that the passing of extrinsic information needs to be carefully managed in order to yield a good decoding result.

The decoding procedure is depicted in Fig. 4. In the diagram,  $r$  is the received signal,  $P_i(\cdot)$  and  $P_o(\cdot)$  represent the input and output probability vectors of a decoder, respectively, and  $P^e(\cdot)$  represents an *extrinsic* probability vector. The *a priori* probability  $P_i(C^I)$  is computed using  $r$ . The initial value for  $P_i(U^I)$  is a vector of  $1/2$ . These two pieces of information are fed into the CPM APP decoder which produces the extrinsic probability  $P_o^e(U^I)$ . This information is deinterleaved to produce the probability  $P_i(C^o)$ . The probability  $P_i(U^o)$  is set to be a vector of  $1/2$  (unless  $U^o$  is known to be biased). The two probabilities,  $P_i(C^o)$  and  $P_i(U^o)$ , now act as the *a priori* information for the PCCC APP Decoder which produces two outputs,  $P_o^e(C^o)$  and  $P_o(U^o)$ . The former is interleaved to give the probability  $P_i(U^I)$  so that iterative decoding can continue.

The PCCC APP Decoder, which is inside the dashed box in Fig. 4, is detailed in Fig. 5. There are two constituent decoders, DEC1 and DEC2, which correspond to the two constituent encoders. The extrinsic information from the CPM APP Decoder, i.e., the probability vector  $P_o^e(U^I)$ , is first deinterleaved to separate the systematic and parity components, i.e.,  $P_i(C_s^o)$ ,  $P_i(C_{p1}^o)$  and  $P_i(C_{p2}^o)$ . The first probability vector,  $P_i(C_s^o)$ , is then multiplied by the deinterleaved probability vector  $P_o^e(C_s^o)$ , which is the extrinsic information from DEC2

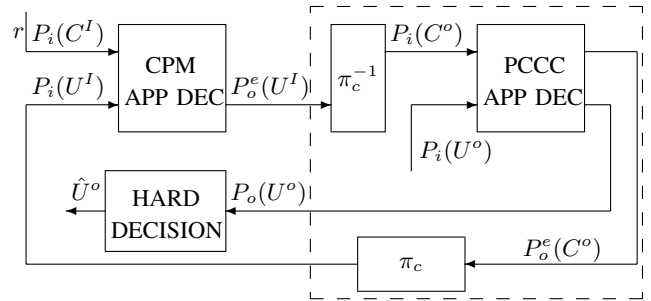


Fig. 4. Iterative soft decision decoding

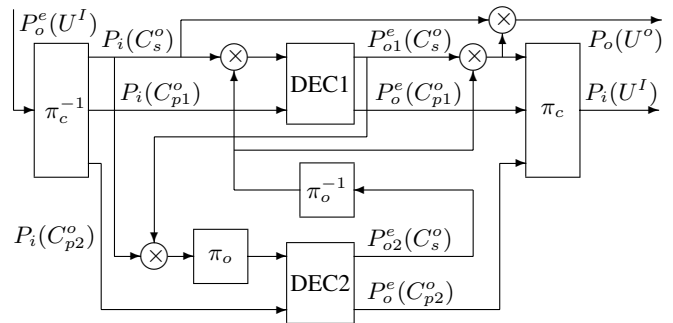


Fig. 5. Iterative soft decision decoding: The PCCC part

in the previous iteration. This result and the probability vector  $P_i(C_{p1}^o)$ , acting as the *a priori* information for DEC1, are fed into DEC1 to give the extrinsic information, i.e., the two probability vectors  $P_o1^e(C_s^o)$  and  $P_o^e(C_{p1}^o)$ . The decoder DEC2 works in a similar way. Then,  $P_o1^e(C_s^o)$  and the deinterleaved  $P_o2^e(C_s^o)$  are multiplied together. The result is combined together with  $P_o^e(C_{p1}^o)$  and  $P_o^e(C_{p2}^o)$  and they are interleaved to produce  $P_i(U^I)$  which is the *a priori* information about  $U^I$  for the CPM APP Decoder in the next iteration. By one iteration we mean that the extrinsic information passes through the three constituent decoders without repeat.

## IV. SIMULATIONS AND COMPARISONS

The proposed scheme in Fig. 2 has been simulated for the AWGN channel. The constituent encoder of the PCCC is a 2-state non-recursive encoder with generator polynomial  $[1, 1 + D]$  or  $(2, 3)$  in octal representation while the inner encoder is a 8-state multi-alphabet binary CPM as described earlier. The parity bit sequences of the PCCC are punctured to give the coding rate  $R_o = 1/2$ . Coherent demodulations are assumed. The input block length is 1024 and 10 iterations are used (further iterations will only give negligible improvements). The simulation result is shown in Fig. 6 (the lowest curve).

For comparison purposes, we have also simulated schemes A, B, E, F. The simulation result of scheme D is shown in Fig. 7. It is clear from Fig. 6 and Fig. 7 that the proposed scheme has the best performance. This is in line with our earlier EXIT chart analysis.

Fig. 7 also compares the simulation result of the proposed scheme with those published in [5], [8] and [10]. The scheme



in [5] is same with scheme D. Note that both [5] (Moqvist) and [8] (Narayanan) use the (7, 5) (octal) code as the outer code and MSK as the inner code, whereas [10] (two channel approach) uses two convolutionally coded CPM channels. All the schemes consume comparable bandwidths with the same coding rate and input block length. We observe that the proposed scheme outperforms the schemes in [5] and [8] by about 0.5 dB at BER of  $10^{-5}$ . When compared with [10], our scheme also gives 0.2 dB improvement at BER of  $10^{-5}$ . However, we recall that the result of [10] is achieved using two CPM channels whereas others use only one CPM channel.

We may also analyze the decoding complexity by comparing the numbers of overall decoding states in different schemes. The scheme in [10] has overall 16 states (8 states for each channel) in decoding complexity and those in [5] and [8] have 6 states (4 in the outer decoder and 2 in the inner decoder). The proposed scheme has an overall 12 states for decoding complexity. Therefore, the proposed scheme achieves the performance improvement at a somewhat higher decoding complexity than [5], [8] (but lower than the scheme in [10]).

## V. CONCLUSION

In this paper, we have shown the advantages of using a parallel concatenated convolutional code (PCCC) and a multi-alphabet binary CPM as an outer code and an inner code, respectively, for serial concatenated binary CPM systems. Our simulations show that, in the concatenation where the modulator contains a recursive encoder such as CPM, using a generic PCCC as an outer code may be inadequate. Instead, careful design of the individual components is required to make the concatenation work effectively. The key design rules are summarized as follows. Firstly, in the serial concatenation with binary CPM as the inner code, non-recursive constituent codes for the PCCC perform better than recursive codes at low signal-to-noise ratio. Secondly, the multi-alphabet binary CPM proposed in this paper gives an improved performance than MSK in the concatenation. Thirdly, the concatenation should avoid correlating the outer codewords from the two constituent encoders.

## REFERENCES

- [1] J. B. Anderson, T. Aulin and C. E. Sundberg, *Digital Phase Modulation*, Plenum, New York, 1986.
- [2] J. G. Proakis, *Digital Communications*, 4th ed., McGraw Hill, 2001.
- [3] B. E. Rimoldi, "A decomposition approach to CPM," *IEEE Trans. Inform. Theory*, vol. 34, no. 3, pp. 260-270, 1988.
- [4] B. E. Rimoldi and Q. Li, "Coded continuous phase modulation using ring convolutional codes," *IEEE Trans. Commun.*, vol. 43, no. 11, pp. 2714-720, 1995.
- [5] P. Moqvist and T. Aulin, "Serially concatenated continuous phase modulation with iterative decoding," *IEEE Trans. Commun.*, vol. 49, no. 11, pp. 1901-1915, 2001.
- [6] S. Benedetto, D. Divsalar, G. Montorsi and F. Pollara, "Serial concatenation of interleaved codes: performance analysis, design, and iterative decoding," *IEEE Trans. Inform. Theory*, vol. 44, pp. 909-926, 1998.
- [7] S. Benedetto, D. Divsalar, G. Montorsi and F. Pollara, "A soft-input soft-output APP module for iterative decoding of concatenated codes," *IEEE Commun. Lett.*, vol. 1, pp. 22-24, 1997.
- [8] K. R. Narayanan and G. L. Stüber, "Performance of trellis-coded CPM with iterative demodulation and decoding," *IEEE Trans. Commun.*, vol. 49, no. 4, pp. 676-687, 2001.

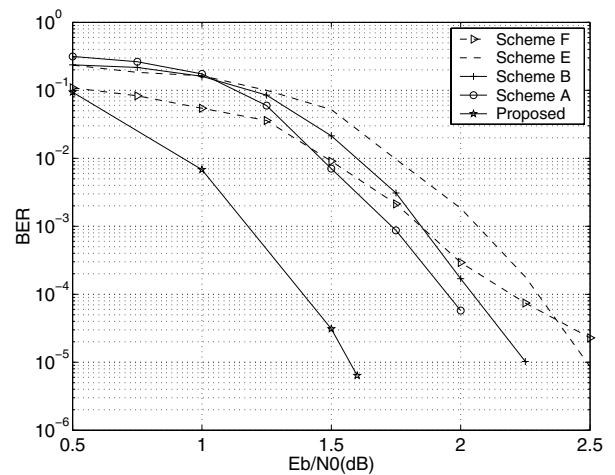


Fig. 6. Performance for different combinations of inner and outer encoders

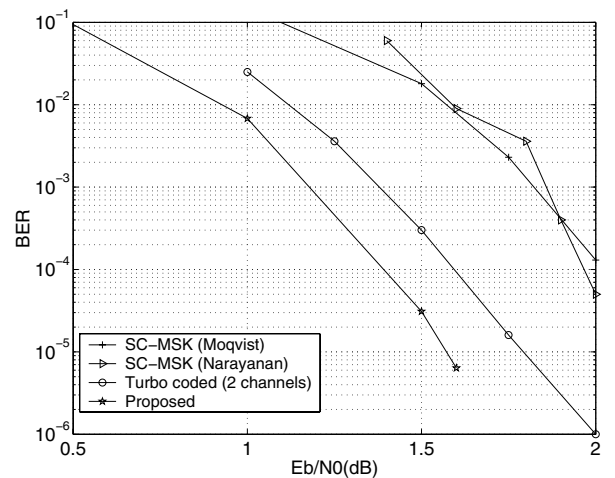


Fig. 7. Performance for the proposed scheme and schemes in [5], [8], [10]

- [9] C. Berrou and A. Glavieux, "Near optimum error correcting coding and decoding: Turbo codes," *IEEE Trans. Comm.*, vol. COM-44, no. 10, pp. 1261-1271, 1996.
- [10] M. R. Shane and R. D. Wesel, "Parallel concatenated turbo codes for continuous phase modulation," in *Proc. IEEE Wireless Commun. and Networking Conf., WCNC*, vol. 1, pp. 147-152, Sept. 2000.
- [11] Stephen G. Wilson and Richard C. Gaus, "Power Spectra of Multi-h phase codes," *IEEE Trans. Commun.*, vol. 29, no. 3, pp. 250-256, 1981.
- [12] A. Z. Yilmaz and W. E. Stark, "Turbo coded continuous phase modulation," in *Proc. Military Commun. Conf.*, vol. 2, pp. 1405-1409, Oct. 2001.
- [13] B. A. Dave and R. K. Rao, "Generalized asymmetric multi-h phase-coded modulation for M-ary data transmission," in *Proc. Canadian Conf. Elect. and Comp. Engr.*, 2004, vol. 1, pp. 559-562, May 2004.
- [14] M. Xiao and T. M. Aulin, "Serially concatenated continuous phase modulation with symbol interleavers: performance, properties and design principles," in *Proc. IEEE GlobeCom*, vol. 1, pp. 179 - 183, Dec. 2004.
- [15] S. ten Brink, "Convergence behavior of iteratively decoded parallel concatenated codes," *IEEE Trans. Commun.*, vol. 49, no. 10, pp. 1727-1737, Oct. 2001.
- [16] S. ten Brink, "Designing iterative decoding schemes with the extrinsic information transfer chart," in *Proc. AEU Int. J. Electron. Commun.*, vol. 54, pp. 389-398, Feb. 2001.
- [17] B. Scanavino, G. Montorsi and S. Benedetto, "Convergence properties of iterative decoders working at bit and symbol level," in *Proc. IEEE GlobeCom*, vol. 2, pp. 1037-1041, Nov. 2001.